Korean Journal of Remote Sensing, Vol.20, No.1, 2004, pp.39~46

Comparative Evaluation of Two Analytical Models for Microwave Scattering from Deciduous Leaves

Yi-Sok Oh

School of Electronic and Electrical Engineering, Hongik University, Seoul, Korea

Abstract : The generalized Rayleigh-Gans (GRG) approximation is usually used to compute the scattering amplitudes of leaves smaller or comparable to a wavelength, while the physical optics (PO) approach with the resistive sheet approximation is commonly used for leaves larger or comparable to the wavelength. In this paper, the scattering amplitudes of an elliptical leaf are computed using those theoretical scattering models (GRG and PO) at different frequencies. The accuracies of the analytical models for microwave scattering from deciduous leaves are investigated by comparison with the precise estimation by the method of moment (MoM). It was found that both the PO approach and the GRG approximation can be used alternatively for computing the scattering matrices of natural deciduous leaves at P-, L-, C- and X-band frequencies.

Key Words : Scattering Matrix, Generalized Rayleigh-Gans Approximation, Physical Optics Approach.

1. Introduction

Radar scattering from a vegetation canopy can be calculated using the vector radiative transfer (VRT) method (Ulaby *et al*. 1990; Karam *et al*. 1992). It is necessary to compute precisely the scattering matrices of leaves at microwaves to compute the phase and extinction matrices of the crown layer. A deciduous leaf is modeled in (Ulaby *et al*. 1990) as a randomly oriented dielectric resistive sheet using the PO approach (Senior *et al*. 1987). Thus, only leaves larger than a wavelength are considered in the approach, and the simple Rayleigh approximation is applied for smaller leaves. On the other hand, the scattering matrix for a leaf is obtained in (Karam *et al*. 1992) by applying the GRG approximation (Karam *et al*. 1988). The GRG approximation holds only for leaves smaller or comparable to the wavelength. The main objective of this study is to find the valid frequency regions of the PO and the GRG approximations for a given leaf size in order to compute the scattering matrices of leaves accurately.

The interior field in the PO approach is assumed to be the same as that of an infinite disk, which is only valid at high microwave frequencies for natural leaves. In the GRG approach, the electric field inside the dielectric disk is approximated by the incident electric field, which is valid in low microwave frequencies. It was shown in (Pan and Narayanan, 2002) that the difference between these two models is of the order of several dB at L- and X-bands for a circular disk with a radius of 5 cm. The

Received 26 December 2003; Accepted 26 January 2004.

frequency limitations of the analytic scattering models need to be examined for dielectric disks having dimensions of natural leaves.

In this paper, the GRG and PO approximations for an elliptical dielectric disk are reviewed inceptively. Then, a full-wave analysis with the MoM (Oh *et al*., 2002) is performed to examine the accuracies of the analytical scattering models. A typical oak leaf may be compared with an ellipse carrying a major axis of $2a$ = 12 cm and a minor axis of $2b$ = 5 cm. The lengths of the leaf in the major and minor axes are comparable to the wavelengths at 2.5 GHz and 6 GHz, respectively. The angular scattering behaviors of the leaf at various microwave frequencies will be computed using the analytical models (the PO, the GRG, and the Rayleigh approximations). The leaf is assumed to be a dielectric elliptical disk with a thickness t of 0.04 cm. The dielectric constants of the leaf, corresponding to the gravimetric moisture content of 0.6 g/cm^3, are obtained from an empirical formula in (Ulaby and El-Rayes, 1987) for given frequencies.

Fig. 1 shows a coordinate system of the scattering problem with a plane wave incidence on an elliptical dielectric disk lying on the x-y plane, which is the forward scattering assignment (FSA) as in (Ulaby and Elachi, 1990). In the FSA, $\hat{k}_i = \sin\theta_i\cos\phi_i\hat{x} + \sin\theta_i\sin\phi_i\hat{y} + \cos\theta_i\hat{z}$, $\hat{h}_i = \hat{z}\times\hat{k}_i / |\hat{z}\times\hat{k}_i|$, $\hat{v}_i = \hat{h}_i\times\hat{k}_i$, and $(\hat{v}_s, \hat{h}_s, \hat{k}_s)$ can be obtained from $(\hat{v}_i, \hat{h}_i, \hat{k}_i)$ by substituting *s*'s into *i*'s.

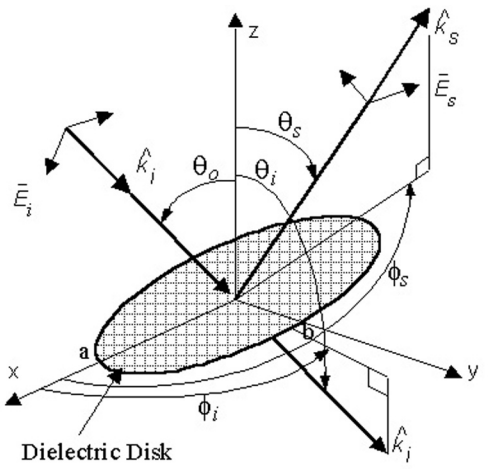

Fig. 1. Geometry of the scattering problem.

A volume current density $\bar{J}(\bar{r})$ is induced in the dielectric disk with an incident electric field of

$$\bar{E}^i(\bar{r}) = \hat{q}_i E_0 e^{ik\hat{k}_i\cdot\bar{r}}, \tag{1}$$

where $\hat{q}_i = \hat{v}_i$ or $\hat{h}_i$, k is the wavenumber and a time convention of $\exp[-i\omega t]$ is assumed. Then, the electric fields scattered from the dielectric body are computed using the electric current density $\bar{J}(\bar{r}')$ and the dyadic Green's function $\bar{\bar{G}}(\bar{r},\bar{r}')$ by

$$\bar{E}^s(\bar{r}) = ik_0\eta_0\int_V \bar{\bar{G}}(\bar{r},\bar{r}')\cdot\bar{J}(\bar{r}')dv'. \tag{2}$$

where $k_0 = 2\pi/\lambda_0$ and $\eta_0 = \sqrt{\mu_0/\varepsilon_0}$. The dyadic Green's function satisfies the wave equation (Tai, 1997),

$$\nabla\times\nabla\times\bar{\bar{G}}(\bar{r},\bar{r}') - k^2\bar{\bar{G}}(\bar{r},\bar{r}') = \bar{\bar{I}}\,\delta(\bar{r}-\bar{r}'), \tag{3}$$

where

$$\bar{\bar{G}}(\bar{r},\bar{r}') = \left(\bar{\bar{I}} + \frac{\nabla\nabla}{k^2}\right)G(\bar{r}-\bar{r}') \text{ and} \tag{4}$$

$$G(\bar{r},\bar{r}') = \frac{e^{ik|\bar{r}-\bar{r}'|}}{4\pi|\bar{r}-\bar{r}'|}. \tag{5}$$

In the far zone, the scattered fields can be calculated with the following approximated equations:

$$\bar{\bar{G}}(\bar{r},\bar{r}') \approx (\hat{v}_s\hat{v}_s + \hat{h}_s\hat{h}_s)G(\bar{r}-\bar{r}') \text{ and} \tag{6}$$

$$G(\bar{r},\bar{r}') \approx \frac{e^{ikr}}{4\pi r}e^{-ik\hat{k}_s\cdot\bar{r}'}. \tag{7}$$

The current densities $\bar{J}(\bar{r}')$ in the dielectric disk are obtained in a simple form with appropriate assumptions for the analytical models (the Rayleigh, the GRG, and the PO approximations) as formulated in Section 2, while the $\bar{J}(\bar{r}')$ is computed precisely applying the MoM on an integral equation derived by using (2), (4) and (5) for a full-wave analysis as formulated in Section 3. Then, the scattered fields are computed using (2), (6) and (7) for the analytical and numerical models. In

Section 4 the radar cross sections (RCS) σ of the leaf are computed by the analytical models and compared with the RCS by the full-wave method. The accuracy of each analytical model is investigated in microwave frequencies using the precise numerical results.

The scattered field vector is related to the incident field vector in terms of a dyadic scattering amplitude $\overline{\overline{S}}$ as follows:

$$\overline{E}^s(\overline{r}) = \frac{e^{ikr}}{r}\overline{\overline{S}}(\hat{k}_s, \hat{k}_i)\cdot\hat{q}_i E_0 \tag{8}$$

where the scattering amplitude S_{pq} for a q-polarized incident wave and a p-polarized scattered wave can be written by

$$S_{pq} \equiv \hat{p}_s \cdot \overline{\overline{S}}(\hat{k}_s, \hat{k}_i)\cdot\hat{q}_i. \tag{9}$$

Then, the RCS of the dielectric disk is computed by

$$\sigma_{pq} = 4\pi |S_{pq}|^2, p, q = v, h. \tag{10}$$

From the Maxwell equations, we get the equivalent volume current $\overline{J}(\overline{r}')$ in the dielectric disk as

$$\overline{J}(\overline{r}') = -i\omega\varepsilon[\varepsilon_r - 1]\overline{E}(\overline{r}'), \tag{11}$$

where ε_r is the complex dielectric constant of the disk and $\overline{E}(\overline{r}')$ is the total electric field including the incident and scattered fields.

2. Full-wave Analysis

In (11) the total electric field comprises the incident and scattered fields, $\overline{E} = \overline{E}^i + \overline{E}^s$. Therefore, an integral equation can be obtained by substituting (2) into (11) as

$$\overline{J}(\overline{r}) - k_0^2(\varepsilon_r - 1)\int_V \overline{\overline{G}}(\overline{r}, \overline{r}')\cdot\overline{J}(\overline{r}')dv' = -i\omega\varepsilon(\varepsilon_r - 1)\overline{E}^i(\overline{r}). \tag{12}$$

The unknown current density $\overline{J}(\overline{r})$ in the leaf can be computed numerically using the method of moment (MoM). Among many other bases functions, the volumetric brick was chosen as the basis function in the limit of electrically small subdomains for simplicity. Using the point matching technique, the integral equation (12) can be cast into the following matrix equation,

$$\begin{pmatrix} [Z_{mn}^{xx}] & [Z_{mn}^{xy}] & [Z_{mn}^{xz}] \\ [Z_{mn}^{yx}] & [Z_{mn}^{yy}] & [Z_{mn}^{yz}] \\ [Z_{mn}^{zx}] & [Z_{mn}^{zy}] & [Z_{mn}^{zz}] \end{pmatrix} \begin{pmatrix} [I_n^x] \\ [I_n^y] \\ [I_n^z] \end{pmatrix} = \begin{pmatrix} [V_m^x] \\ [V_m^y] \\ [V_m^z] \end{pmatrix}, \tag{13}$$

where I_n^p is an unknown constant of the nth basis function for the p-component of the volume currents ($p = x, y, z$), and

$$V_m^p = -i\omega\varepsilon_0[\varepsilon_r(\overline{r}_m) - 1]\hat{q}\, e^{ik_0\hat{k}_i\cdot\overline{r}_m}\cdot\hat{p}, p = x, y, z \tag{14}$$

$$Z_{mn}^{pq} = \delta_{pq}\delta_{mn} - k_0^2[\varepsilon_r(\overline{r}_m) - 1]\int_{\Delta V_n} G_{pq}(\overline{r}_m, \overline{r}_n)dv_n, p, q = x, y, z. \tag{15}$$

where δ_{pq} and δ_{mn} are the Kronecker delta functions, and $\overline{r}_m$ and $\overline{r}_n$ represent the mth matching position (observation point) and the nth integration position, respectively. The elements of the dyadic Green's function are found to be

$$G_{pp}(\overline{r}_m, \overline{r}_n) = G(R) + \frac{1}{k_0^2}\frac{\partial^2 G(R)}{\partial p^2}, \tag{16a}$$

$$G_{pq}(\overline{r}_m, \overline{r}_n) = \frac{1}{k_0^2}\frac{\partial^2 G(R)}{\partial p \partial q}, p \neq q, \tag{16b}$$

where $p, q = x, y, z$ and $R = |\overline{r}_m - \overline{r}_n|$. Explicit form of differentiations of the Green's functions in (16) are given by

$$\frac{\partial^2 G(R)}{\partial p^2} = G(R)\left\{\frac{P_{mn}^2 f_1}{R^4} - \frac{(1 - ik_0 R)}{R^2}\right\}, \tag{17a}$$

$$\frac{\partial^2 G(R)}{\partial p \partial q} = G(R)\frac{P_{mn}q_{mn}f_1}{R^4}, p \neq q, \tag{17c}$$

where $p, q = x, y, z$, $p_{mn} \equiv p_m - p_n$, $q_{mn} \equiv q_m - q_n$, and $f_1 = 3 - i3k_0R - k_0^2R^2$.

When $n = m$, the second derivatives of the Green's function $G(R)$ produces the well-known singularity. However, we can avoid this singularity by introducing an auxiliary function $g \equiv 1/4\pi R$ and subdividing the integral region to a small sphere V_ε centered at the

observation point and the other part as in (Oh *et al*., 2002):

$$\int_{\Delta V_n} G_{pp} dv = \int_{\Delta V_n - V_\varepsilon} G_{pp} dv + \int_{V_\varepsilon} G dv + \frac{1}{k_0^2}\left[\int_{V_\varepsilon} \frac{\partial^2}{\partial p^2}(G-g)dv + \int_{V^\varepsilon} \frac{\partial^2}{\partial p^2} g\, dv\right]. \quad (18)$$

We can evaluate the integrals in the parenthesis in (18) explicitly for a small sphere with radius a, which leads to $-(1-ika)e^{ika}/3$. The integral of the second term in (18) can also be explicitly evaluated, and leads to $\{-1+(1-ika)e^{ika}\}/k_0^2$. Therefore, (18) becomes

$$\int_{\Delta V_n} G_{pp} dv_n = \int_{\Delta V_n - V_\varepsilon} G_{pp} dv_n + \frac{1}{k_0^2}\left\{-1 + \frac{2}{3}(1-ika)e^{ika}\right\} \quad (19)$$

where $p = x, y, z$. The first integral of the right side of (19) was evaluated using a numerical integration technique.

Once the elements of the impedance matrix [Z] and the excitation vector [V] were calculated, the unknown equivalent volume current [I] inside the dielectric body can be found by inverting (13). Consequently, the scattering amplitude S_{pq} can be computed using (2) and (6)-(9).

3. Analytical Models

In this section, the Rayleigh, the generalized Rayleigh-Gans (GRG), and the physical optics (PO) models are formulated based on the equations in the previous section with appropriate assumptions. For the Rayleigh approximation, the internal field within the dielectric disk is assumed to be the same as the incidence field, and the phase interference of the scattering is omitted, assuming the leaf size is much less than a wavelength ($ka \ll 1$). The GRG model is same to the Rayleigh approximation except that the phase term is retained within the integral, and the phase interference function works as a modifying factor (Karam *et al*. 1988). For the PO approximation, the edge effect is ignored assuming the leaf size is much greater than a wavelength. Moreover, the leaf can be assumed to be a resistive sheet assuming the leaf is very thin (Senior *et al*. 1987).

1) Rayleigh Approximation

Assuming the disk is very small, relative to a wavelength, the field inside the disk is approximated to the incident field $\bar{E}^i(\bar{r}')$ in (11).

The scattering amplitude is given in (Karam and Fung, 1989) as follows:

$$S_{pq} = \hat{p}_s \cdot \frac{k^2}{4\pi}(\varepsilon_r - 1)\left(\hat{v}_s\hat{v}_s + \hat{h}_s\hat{h}_s\right) \cdot \bar{\bar{\mathrm{A}}} \cdot \hat{q}_i v_0, \quad (12)$$

where v_0 is the leaf volume and $\bar{\bar{\mathrm{A}}}$ is the polarizability tensor (Tsang *et al*. 1985) given as

$$\bar{\bar{\mathrm{A}}} = \frac{\hat{x}\hat{x}}{1+(\varepsilon_r-1)g_1} + \frac{\hat{y}\hat{y}}{1+(\varepsilon_r-1)g_2} + \frac{\hat{z}\hat{z}}{1+(\varepsilon_r-1)g_3}. \quad (21)$$

The demagnetizing factor g_i's can be written for an elliptic disk-shaped leaf ($a>b>>t/2$) as

$$g_1 = \frac{t}{2a}\sqrt{1-e^2}\,\frac{K(e)-E(e)}{e^2}, \quad (22a)$$

$$g_2 = \frac{t}{2a}\,\frac{E(e)-(1-e^2)K(e)}{e^2\sqrt{1-e^2}}, \text{ and} \quad (22b)$$

$$g_3 = 1 - \frac{t}{2a}\,\frac{E(e)}{\sqrt{1-e^2}}, \quad (22c)$$

with $e = \sqrt{1-(b/a)^2}$.

$K(e)$ and $E(e)$ are the elliptic integrals of the first and second kind, respectively, and can be written in polynomial approximation as in (Abramowitz and Stegan, 1972):

$$K(e) \approx [a_0 + a_1 e + \cdots + a_4 e^4] + [b_0 + b_1 e + \cdots + b_4 e^4]\ln(1/e), \quad (23a)$$

$$E(e) \approx [1 + c_1 e + \cdots + c_4 e^4] + [d_1 e + \cdots + d_4 e^4]\ln(1/e), \quad (23b)$$

where the constants, $a_0, \cdots, a_4, b_0, \cdots, b_4, c_1, \cdots, c_4, d_1, \cdots, d_4$, are given in (Abramowitz and Stegan, 1972).

2) GRG Approximation

The GRG approximation may be applied for a small scatterer satisfying $kD(\varepsilon_r - 1) \ll 1$, where D is the smallest dimension of the scatter. In the GRG approximation, the total electric field $\bar{E}(\bar{r})$ is also approximated by the incident electric field $\bar{E}^i(\bar{r})$, and the integral factor with $\exp[ik(\hat{k}_i - \hat{k}_s)\cdot\bar{r}']$ is kept. Thus, the scattering amplitude is same with that of the Rayleigh approximation except the modifying factor $M(\hat{k}_s - \hat{k}_i)$:

$$S_{pq} = \hat{p}_s \cdot \frac{k^2}{4\pi}(\varepsilon_r - 1)(\hat{v}_s\hat{v}_s + \hat{h}_s\hat{h}_s)\cdot\bar{\bar{\mathrm{A}}}\cdot\hat{q}_i M(\hat{k}_s, \hat{k}_i), \quad (24)$$

where

$$M(\hat{k}_s, \hat{k}_i) = \int_V e^{ik(\hat{k}_i - \hat{k}_s)\cdot\bar{r}'} dv'. \quad (25)$$

Ignoring the phase variation in $\hat{z}$ -direction because of the condition $a > b \gg t$, the modifying factor becomes

$$M(\hat{k}_s, \hat{k}_i) = t\int_S e^{ik_x x' + ik_y y'} dx'\,dy' = tm(\hat{k}_s, \hat{k}_i), \quad (26)$$

where t is the thickness of the disk, $k_x = k(\hat{k}_i - \hat{k}_s)\cdot\hat{x}$ and $k_y = k(\hat{k}_i - \hat{k}_s)\cdot\hat{y}$. The above integral can be simplified by using the integral transformation with $x' = a\lambda\cos\psi$, $y' = b\lambda\sin\psi$, $0 \le \lambda \le 1$, and $0 \le \psi \le 2\pi$. The integral can be further simplified using the wave transformation with summation of the Bessel functions as in (Karam *et al*. 1988):

$$M(\hat{k}_s, \hat{k}_i) = 2\pi abt\int_0^1 J_0(Q\lambda)\lambda d\lambda = 2\pi abt\frac{J_1(Q)}{Q}, \quad (27)$$

where $Q = \sqrt{(k_x a)^2 + (k_y b)^2}$.

3) The PO Approximation

Assuming the leaf as a resistive sheet, the equivalent current $\bar{J}(\bar{r}')$ in (2) can be approximated to a surface current distribution $\bar{J}_s^R(\bar{r}')$ on the resistive sheet lying on x-y plane as

$$\bar{J}_s^R(\bar{r}') = \bar{J}_s^{pc}(\bar{r}')\Gamma_q. \quad (28)$$

The PO surface current on a perfect conductor $\bar{J}_s^{pc}(\bar{r}')$ can be obtained using the equivalence principle as

$$\bar{J}_s^{pc}(\bar{r}') = 2\hat{z}\times\bar{H}_0 e^{ik\hat{k}_i\cdot\bar{r}'} \quad (29)$$

where $\bar{H}_0 = \hat{k}_i \times \hat{q}_i\, E_0/\eta_0$. The horizontal and vertical reflection coefficients (Γ_h and Γ_v) for a resistive sheet can be derived using the impedance boundary conditions as in (Senior *et al*., 1987):

$$\Gamma_h = \left(1 + \frac{2R\cos\theta_0}{\eta_0}\right)^{-1} \text{ and} \quad (30a)$$

$$\Gamma_v = \left(1 + \frac{2R}{\eta_0\cos\theta_0}\right)^{-1}, \quad (30b)$$

with

$$R = \frac{i\eta_0}{k_0 t(\varepsilon_r - 1)} \quad (31)$$

where R is the resistivity of the leaf, $\theta_0 = \pi - \theta_i$, and t is the leaf thickness.

Substituting (29) into (28), the current distribution is written as

$$\bar{J}_s^R(\bar{r}') = \frac{2E_0}{\eta_0}\left[\hat{z}\times(\hat{k}_i\times\hat{q}_i)\right]\Gamma_q e^{ik\hat{k}_i\cdot\bar{r}'} \quad (32)$$

where $q = v$ or h. Then, the scattering amplitude for a $\hat{q}$-polarized incident wave and a $\hat{p}$-polarized scattered wave is given as

$$S_{pq} = \hat{p}_s \cdot \frac{ik}{2\pi}(\hat{v}_s\hat{v}_s + \hat{h}_s\hat{h}_s)\cdot\left[\hat{z}\times(\hat{k}_i\times\hat{q}_i)\right]\Gamma_q m(\hat{k}_s, \hat{k}_i), \quad (33)$$

where the phase interference function $m(\hat{k}_s, \hat{k}_i)$ is given in (26) and (27). For example, S_{vh} can be computed by substituting $\hat{h}_i$ into $\hat{q}_i$ and $\hat{v}_s$ into $\hat{p}_s$ presented in (33).

4. Numerical Results

The backscatter and forward-scatter radar cross sections (RCS) are computed for a typical deciduous leaf for various frequencies and angles. The leaf is an elliptical disk with a major axis of $2a$ = 12 cm, a minor axis of $2b$ = 5 cm, a thickness t = 0.04 cm (Fig. 1). The gravimetric moisture content of the leaf is assumed to be 0.6 g/cm^3, and the corresponding complex dielectric constants for given frequencies are computed using an empirical formula given in (Ulaby and El-Rayes, 1987). For example, the complex dielectric constant of the leaf at 5.3 GHz is (19.20, 6.42).

The backscattering cross sections of the leaf were computed using the Rayleigh, the GRG and the PO approximations as well as the MoM at 9.6 GHz (which is the frequency for the X-band SAR system of the SIR-C mission) for VV-polarization over the range $0^\circ \leq \theta \leq 90^\circ$ as shown in Fig. 2. In the computation, the cell size of the elliptical dielectric disk for the MoM was 0.25 cm × 0.25 cm ($\lambda/12.5 \times \lambda/12.5$) and the number of the cell was 741 in this case. It was known that the GRG approximation holds for leaf surface dimension smaller or comparable to the wavelength. Fig. 2, however, shows that the GRG approximation is as good as the PO approximation for a leaf with a leaf-length of 3.84λ. It is obvious that the Rayleigh approximation is not applicable for a leaf larger than a wavelength as shown in Fig. 2, because of ignoring the modifying factor of (25).

Fig. 3 shows the backscattering cross sections of the dielectric disk, which are computed using the analytical models and the MoM at 0.44 GHz. In the MoM computation the cell size was 0.4 cm × 0.4 cm ($\lambda/170 \times \lambda/170$), which gives the number of cell N = 297. The length of the leaf is 0.176λ(= $\lambda/5.68$) at 0.44 GHz (which is the frequency for the P-band system of the JPL/NASA Airborne SAR). It was known that the PO approach is inherently a high frequency approximation and therefore should be applied with caution when the size of a dielectric disk is not larger than wavelength (Le Vine, 1984). Fig. 3, however, shows that the PO approach is as good as the GRG approximation for an elliptical dielectric disk with a length of 0.176λ. The Rayleigh approximation agrees with the other models, because the phase variation in the disk is negligible in a very small disk compared with wavelength ($2a$ = 12 cm $\ll \lambda$ = 68.18 cm in this case). It was shown that the PO approximation disagrees with the other models near 90° (near edge-on incidence) because the disk is assumed as a surface-current sheet in the PO approximation.

Fig. 4 shows the forward-scattering cross sections of the leaf, which are computed using the analytical and numerical models at X-band for VV- and HH-polarizations. The incidence wave has $\theta_0 = 60^\circ$ (θ_i = 120°), $\phi_i = 0^\circ$ and the scattered wave has $\phi_s = 0^\circ, 0^\circ \leq \theta_s \leq 180^\circ$ (Fig. 1). The Rayleigh approximation agrees with the GRG approximation only at the incidence angles: *i.e.*, θ_s = 60°, 120°, and deviates from the other models. The GRG approximation agrees very well with the MoM even at 9.6 GHz, especially for VV-polarization as shown in Fig. 4. Fig. 4 also shows that the forward-scattering RCS computed by the PO approach has a null shifted to 90° and has the same RCS at backward direction (θ_s = 60°) with forward direction

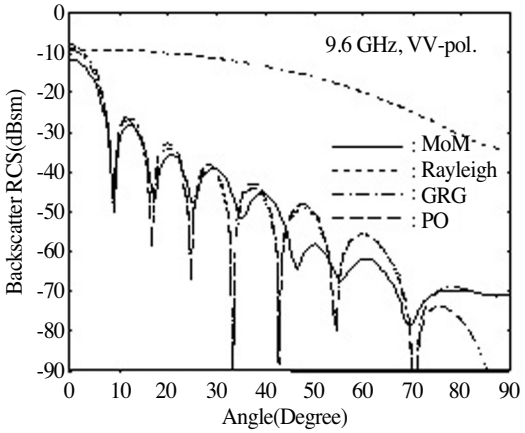

Fig. 2. Comparisons of analytical and numerical backscatter cross sections of a leaf at 9.6 GHz and VV-polarization.

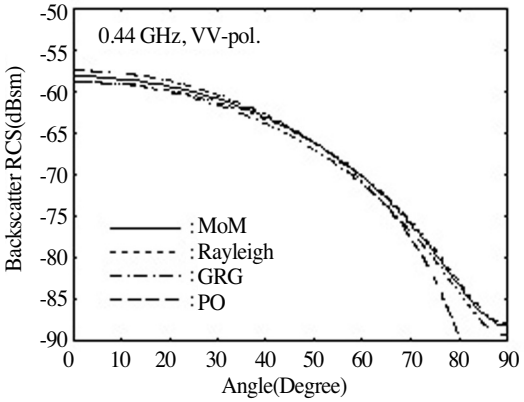

Fig. 3. Comparisons of analytical and numerical backscatter cross sections of a leaf at 0.44 GHz and VV-polarization.

(θ_s = 120°), deviated from the precise results by the MoM. The computation results for HH-polarization are similar to the results for VV-polarization.

Fig. 5 demonstrates that the PO approach is also good for computing the forward-scattering cross section of the leaf even though the dimension of the leaf is very small ($2a = 0.176\lambda$ and $2b = 0.073\lambda$) compared with wavelength at 0.44 GHz. The forward-scattering RCS by the Rayleigh approximation is same to that by the GRG approximation in Fig. 5, because the modifying factor $M(\hat{k}_s, \hat{k}_i)$ is equal to 1 for a very small scatterer. The difference between the PO and the GRG models is about 1 dB for both polarizations, and the forward-scattering cross sections from those models agree well with that from the MoM for VV-polarization, while those are 2~3 dB higher than the MoM for HH-polarization. When we compute the scattering amplitudes of deciduous leaves having various sizes, shapes, and orientations in a crown layer of a vegetation canopy, we may choose either of the PO or the GRG model regardless of the size of the leaves for practical range of microwave frequencies.

Fig. 6 shows the backscattering cross sections at normal incidence ($\theta_0 = \theta_s = 0°, \theta_i = 180°$), for a leaf ($2a$ = 12 cm, $2b$ = 5 cm, t = 0.04 cm) over the frequency range 0.25 GHz $\leq f \leq$ 25 GHz, which corresponds the range of leaf-length $0.1\lambda \leq 2a \leq 10\lambda$. The difference between two models is only about 1dB over the range $0.1\lambda \leq 2a \leq 10\lambda$ as shown in Fig. 6. The angular variations of both models are same, because the modifying factors of both models have the same angular variations as in (24), (26), and (33). This result informs us that the GRG model is as good as the PO model for computation of the scattering amplitudes of leaves 10 times larger than a wavelength, and on the other hand, the PO model is as good as the GRG model for leaves 0.1 times smaller than a wavelength.

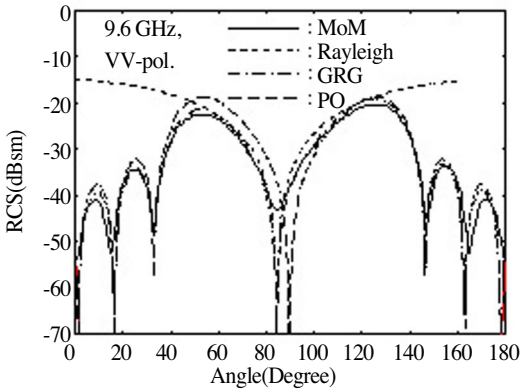

Fig. 4. Comparisons of analytical and numerical forward-scatter cross sections of a leaf at 9.6 GHz and VV-polarization.

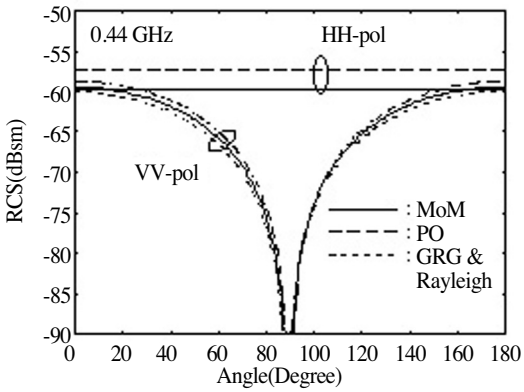

Fig. 5. Comparisons of analytical and numerical forward-scatter cross sections of a leaf at 0.44 GHz.

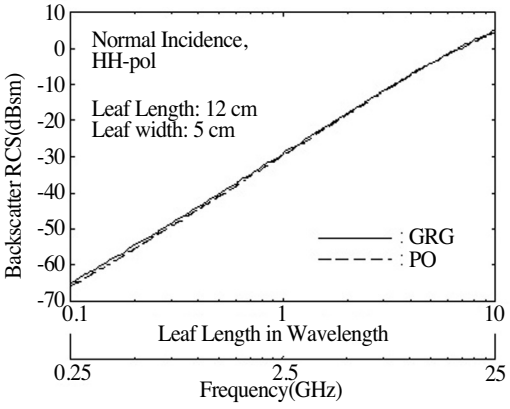

Fig. 6. Variation of the backscatter RCS of a leaf as a function of frequency at normal incidence.

5. Conclusions

The accuracies of the Rayleigh, the GRG, and the PO models for scattering from a leaf were investigated based on the precise numerical results of the MoM. It was known that the GRG model is applicable only for leaves smaller or comparable to a wavelength, while the physical optics (PO) approach for leaves larger or comparable to the wavelength. However, it was found in this study that both the GRG and the PO models could be used for computing the scattering amplitudes of a leaf over the range of length $0.1\lambda \leq 2a \leq 10\lambda$ (or 0.25 GHz $\leq f \leq$ 25 GHz for a leaf with a length of 12 cm). It can be recommended that both the PO and the GRG models be alternatively used for computing the scattering matrices (or the phase matrices) of natural leaves (included in a vegetation canopy) at microwave frequencies.

Acknowledgements:

This work was supported from the Basic Technology Research Support Program (03-Basic-0133) of the Ministry of Information and Communication (Institute of Information Technology Assessment).

References

Abramowitz, M. and I. A. Stegan, 1972. *Handbook of Mathematical Functions*, Dover Publication, Inc., New York.

Karam, M. A., A. K. Fung, and Y. M. M. Antar, 1988. Electromagnetic wave scattering from some vegetation samples, *IEEE Trans. Geosci. Remote Sensing*, 26(6): 799-808.

Karam, M. A. and A. K. Fung, 1989. Leaf-shape effects in electromagnetic wave scattering from vegetation, *IEEE Trans. Geosci. Remote Sensing*, 27(6): 687-697.

Karam, M. A., A. K. Fung, R. H. Lang, and N. S. Chauhan, 1992. A microwave scattering model for layered vegetation, *IEEE Trans. Geosci. Remote Sensing*, 30(4): 767-784.

Le Vine, D. M., 1984. The radar cross section of dielectric disks, *IEEE Trans. Antennas Propag.*, . AP-32(1): 6-12.

Oh, Y., Y-M. Jang, and K. Sarabandi, 2002. Full-wave analysis of microwave scattering from short vegetation: An investigation on the effect of multiple scattering, *IEEE Trans. Geosci. Remote Sensing*, 40(11): 2522-2526.

Pan, G. and R. M. Narayanan, 2002. Comparison of microwave scattering models for leaf, *IEEE Int. Geosci. and Remote Sensing Symp. (IGARSS)*, 1: 653-655.

Senior, T. B. A., K. Sarabandi, and F. T. Ulaby, 1987. Measuring and modeling the backscattering cross section of a leaf, *Radio Science*, 22(6): 1109-1116.

Tai, C. T., 1997. *Generalized Vector and Dyadic Analysis: Applied Mathematics in Field Theory*, 2/e, IEEE Press.

Tsang, L., J. A. Kong, and R. T. Shin, 1985. *Theory of Microwave Remote Sensing*, John Wiley and Sons, New York.

Ulaby, F. T. and M. A. El-rayes, 1987. Microwave dielectric spectrum of vegetation -Part Ⅱ:Dual-dispersion model, *IEEE Trans. Geosci. Remote Sensing*, GE-25: 550-557.

Ulaby, F. T. and C. Elachi, 1990. *Radar Polarimetry for Geoscience Applications*, Artech House, Norwood, MA.

Ulaby, F. T., K. Sarabandi, K. McDonald, M. Whitt, and M. C. Dobson, 1990. Michigan microwave canopy scattering model, *Int. J. Remote Sensing*, 11(7): 1223-1253.